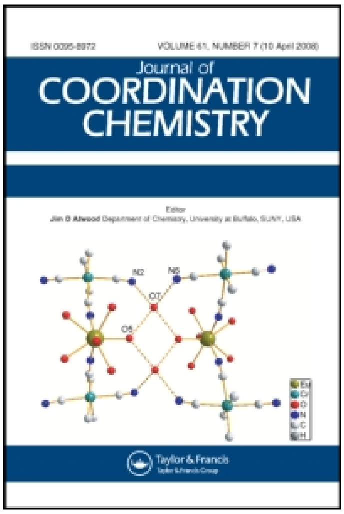

Journal of Coordination Chemistry
Publication details, including instructions for authors and subscription information:
http://www.informaworld.com/smpp/title~content=t713455674

Synthesis and properties of polyaniline doped with iron-substituted silicotungstate isomers with Keggin structure

Ronghua Ma[a]
[a] College of Chemistry and Engineering, Qiqihar University, Qiqihar, China

To cite this Article Ma, Ronghua(2008) 'Synthesis and properties of polyaniline doped with iron-substituted silicotungstate isomers with Keggin structure', Journal of Coordination Chemistry, 61: 7, 1056 — 1065
To link to this Article: DOI: 10.1080/00958970701484772
URL: http://dx.doi.org/10.1080/00958970701484772

Journal of Coordination Chemistry
Vol. 61, No. 7, 10 April 2008, 1056–1065

Taylor & Francis
Taylor & Francis Group

Synthesis and properties of polyaniline doped with iron-substituted silicotungstate isomers with Keggin structure

RONGHUA MA*

College of Chemistry and Engineering, Qiqihar University, Qiqihar 161006, China

(*Received 14 February 2007; in final form 30 March 2007*)

Four polyaniline hybrid materials doped with iron-substituted silicotungstate isomers α, β_i-$K_{5-n}H_n[SiW_{11}Fe(H_2O)O_{39}] \cdot xH_2O$ ($\beta_i = \beta_1$, β_2, β_3) were prepared. The materials were characterized by elemental analysis, IR spectra, UV-Vis spectra, scanning electron microscopy (SEM), TG-DTA and X-ray diffraction (XRD). The conductivity and fluorescence were determined and thermal stability was studied. The UV-Vis, IR and XRD results confirm the existence of Keggin anions. Thermal analysis indicates that $SiW_{11}Fe$/PANI has better thermal stability. The images of scanning electron microscopy (SEM) show that the materials are microporous. The materials exhibit excellent proton conductivity of $8.5 \times 10^{-2}\,S\,cm^{-1}$ at room temperature (20°C). The spectral data indicate that polyaniline doped with α, β_i-$SiW_{11}Fe$ have similar fluorescence, $\lambda_{em} = 418$–$470\,nm$, and emit blue light.

Keywords: Polyaniline; Silicotungstate; Conductivity; Fluorescence; Isomer

1. Introduction

Inorganic–organic hybrid materials receive attention as a result of their specific properties [1, 2]. These new materials have advantages of organic materials, such as light weight, flexibility, and good malleability, and of inorganic materials such as high strength, heat stability and chemical resistance.

Polyaniline is one of the most interesting conducting polymers due to its environmental stability, ease in preparation, exciting electrochemical, optical and electrical properties and possible applications in rechargeable batteries, microelectronic devices, biosensors, electrochromic displays and chemical sensors. The conducting state is usually obtained through p-doping, which takes place with incorporation into the polymer of charge balancing anions. Therefore, aniline polymerizes in the presence of oxidizing agents and under acidic media to yield the protonated/oxidized form of emeraldine in its conducting state. In recent years, research on heteropoly acids (HPA) has been very active [3, 4]. Physical-chemical properties of heteropoly complexes can be modulated by changing their chemical environment by replacing some fragment atoms by transition metal atoms. The Keggin anion α-$SiW_{12}O_{40}^{4-}$ (α-SiW_{12}) is made of four

---

*Tel.: +86-452-2460178 (H); +86-452-2738223 (O). Email: mrh1963@163.com

Journal of Coordination Chemistry
ISSN 0095-8972 print/ISSN 1029-0389 online © 2008 Taylor & Francis
DOI: 10.1080/00958970701484772

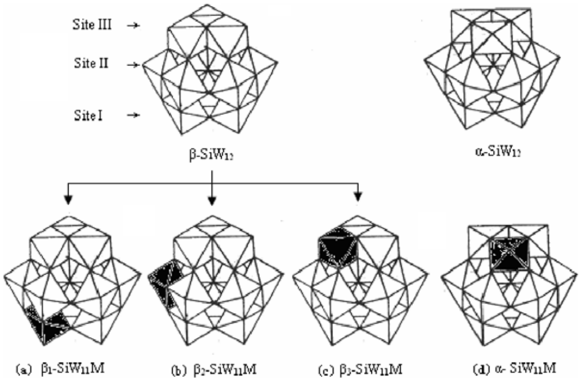

Figure 1. Structures of Keggin anions α, β-SiW_{12} and α, β_1, β_2, β_3-$SiW_{11}M$; black is substituted atom occupation site.

W_3O_{13} groups resulting from sharing of edges of strongly distorted WO_6 octahedra. These groups are associated around a central SiO_4 tetrahedron by sharing vertices. The polyanion thus has T_d symmetry (figure 1). β-$SiW_{12}O_{40}^{4-}$ (β-SiW_{12}) derives from the Keggin structure by rotating a W_3O_{13} group over $\pi/3$ around a threefold axis. The idealized polyanion thus has C_{3v} symmetry (figure 1). As for β-$SiW_{12}O_{40}^{4-}$, there are three forms when the substituted atom in a mono-substituted β-$SiW_{12}O_{40}^{4-}$, is on different positions (figure 1); the substituted atom is in one of three sites of the rotated group (site III), a β_3-isomer (figure 1c); the substituted atom is adjacent to the rotated group (site II), a β_2-isomer (figure 1b); the substituted atom is far from the rotated group (site I), a β_1-isomer (figure 1a) [5]. In this article, we report the preparation of polyaniline doped with iron-substituted silicotungstate isomers. Elemental analysis, IR, UV–Vis, SEM, TG and XRD spectra characterized the polyaniline. The conductivity of the polyaniline doped with α, β_i-$K_{5\text{-}n}H_n[SiW_{11}Fe(H_2O)O_{39}] \cdot xH_2O$ ($\beta_i = \beta_1$, β_2, β_3) was studied and the fluorescence was found.

2. Experimental

2.1. *Instruments and reagents*

All chemicals used were of analytical grade. The aniline used was distilled twice under vacuum. Leeman Lab ICP emission spectrometer and PE2400CHN element analyzer were used. FT-IR studies were carried out on a Spectrum-One FT-IR spectrophotometer with KBr pellets. The UV-Vis absorption spectra were obtained with a Tu-1901 UV spectrophotometer. XRD patterns were taken on a BD90 XJ 10-60N X-ray diffractometer with monochromated Cu-Kα radiation ($\lambda = 0.15418$ nm, power 35 kV × 20 mA). A FEISIRION scanning electron microscope (SEM) was employed to observe the morphology of the hybrid polyaniline/heteropoly acid material. TG measurements were carried out on a SII Pryis Diamond thermal analyzer under a constant nitrogen flow with a scanning rate of $10.0^\circ C\,min^{-1}$. The conductivity was measured using a standard four-probe technique. Disk shape samples were prepared from powders using 20 MPa pressure at room temperature. The photoluminescence spectra were recorded with an F-4500 apparatus.

2.2. *Synthesis*

2.2.1. α, β_i-$K_8[SiW_{11}(H_2O)O_{39}] \cdot xH_2O$ (noted α, β_i-SiW_{11}; $\beta_i = \beta_1, \beta_2, \beta_3$). Were synthesized according to [6] and examined by polarographic and IR spectra.

2.2.2. α, β_i-$K_{5-n}H_n[SiW_{11}Fe(H_2O)O_{39}] \cdot xH_2O$ (noted α, β_i-$SiW_{11}Fe$; $\beta_i = \beta_1, \beta_2, \beta_3$). Were synthesized according to the literature [7]: 6.4 g of α- or β_i-SiW_{11} was dissolved in 30 mL of water, maintained at 40°C, while 4 mL of a 0.5 mol L^{-1} solution of $FeCl_3$ was added dropwise to the solution. The salt was precipitated with 2 g of potassium chloride, filtered and dissolved again in hot water. The potassium salt, which crystallized upon cooling was examined by polarographic and IR spectra.

2.2.3. Polyaniline doped with α, β_i-$SiW_{11}Fe$ (α, β_i-$SiW_{11}Fe$/PANI). Freshly distilled aniline (2 mL) and acetic acid (1 mL) were placed in a mortar and cooled to −20°C for 20 min, then α- or β_i-$SiW_{11}Fe$ (5 g) and $(NH_4)_2S_2O_8$ (3 g) were placed in the mortar, furbishing for ca 30 min. The color of solid changed to black–green and it was then washed with distilled water until pH = 7 was achieved; the powder was dried under vacuum at 50°C for 48 h. According to the results of the elemental analysis, the following empirical formula was obtained. α-$(C_6H_{4.5}N)(SiW_{11}Fe)_{0.1111}$ (analytical found values: W 55.14%, C 15.96%, H 1.66%, N 3.44%); β_1-$(C_6H_{4.5}N)(SiW_{11}Fe)_{0.1106}$ (analytical found values: W 51.58%, C 14.36%, H 1.62%, N 3.25%); β_2-$(C_6H_{4.5}N)(SiW_{11}Fe)_{0.1063}$ (analytical found values: W 55.89%, C 15.77%, H 1.56%, N 3.64%); β_3-$(C_6H_{4.5}N)(SiW_{11}Fe)_{0.1306}$ (analytical found values: W 60.91%, C 15.86%, H 1.56%, N 3.23%).

3. Results and discussion

3.1. *IR spectra*

The IR spectra of the materials are shown in figure 2. The intensity ratio of absorption at 1589 cm^{-1} from the quinoid ring and at 1501 cm^{-1} corresponding to benzene is more than 1 in IR spectra of the polyaniline base; bands in the range 1200–1400 cm^{-1} are C–N stretching bands of an aromatic amine [8]. The characteristic band of polyaniline base is the N=Q=N stretch at 1166 cm^{-1}. The IR spectra change after polyaniline is doped with iron-substituted silicotungstate isomers; the 1589 cm^{-1} band shifts slightly to lower frequency and the 1501 cm^{-1} band is unaffected with the relative intensity ratio of 1589/1501 cm^{-1} decreasing, indicating that doping occurs in –N= with the intensity of the benzene ring increasing and quinonoid ring decreasing. The band at ca 1142 cm^{-1} is characteristic of the protonated state [9], showing that polyaniline has been protonated. Characteristic vibrations of the heteropoly acid in the range 700–1100 cm^{-1}

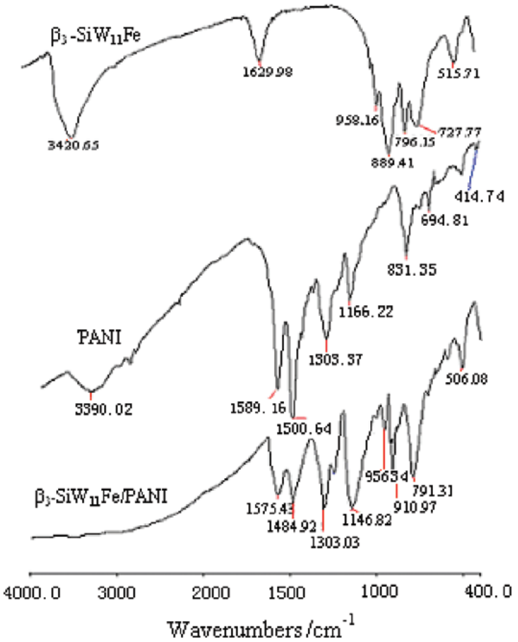

Figure 2. IR spectra of β_3-SiW$_{11}$Fe, β_3-SiW$_{11}$Fe/PANI and PANI base.

Table 1. IR spectra of polyaniline/SiW$_{11}$Fe (cm^{-1}).

Samples	N=Q=N	N–B–N	C–N	Q–NH$^+$–B	W–O$_d$	Si–O$_a$	W–O$_b$–W	W–O$_c$–W
α-SiW$_{11}$Fe/PANI	1574.92	1485.25	1302.91	1145.60	956.14	908.72	878.21	789.94
β_1-SiW$_{11}$Fe/PANI	1568.66	1482.84	1303.77	1143.25	956.14	910.24	878.52	789.90
β_2-SiW$_{11}$Fe/PANI	1575.42	1484.79	1304.17	1146.81	955.96	911.00	878.34	792.47
β_3-SiW$_{11}$Fe/PANI	1575.43	1484.92	1303.03	1146.82	956.54	910.97	879.21	791.31
α-SiW$_{11}$Fe					957.60	902.02	878.21	795.80
β_1-SiW$_{11}$Fe					959.19	903.72	874.25	790.89
β_2-SiW$_{11}$Fe					960.16	899.88	876.22	619.35
β_3-SiW$_{11}$Fe					958.16	889.41	796.15	727.77
PANI	1589.16	1500.64	1303.37	1166.22				

appear [10], indicating that heteropoly acid has gone into polyaniline. The IR frequencies, including assignments of the polyaniline, are listed in table 1.

3.2. *UV–Vis spectra*

Figure 3 shows the UV–Vis absorption spectra of the intrinsic polyaniline and polyaniline doped with α, β_i-SiW$_{11}$Fe. For polyaniline, the band at 630 nm can be attributed to the π_b–π_q^* electronic transition of quinone and benzene [11]. In the polyaniline doped with α, β_i-SiW$_{11}$Fe, two new bands appear at 440 and 850 nm, characteristic of doped states of polyaniline, attributed to the polaron absorption [12]. The intensity at 440 nm is stronger than at 850 nm, indicating that the conductivity of the polyaniline doped with α, β_i-SiW$_{11}$Fe is better [13]. The appearance of the polaron

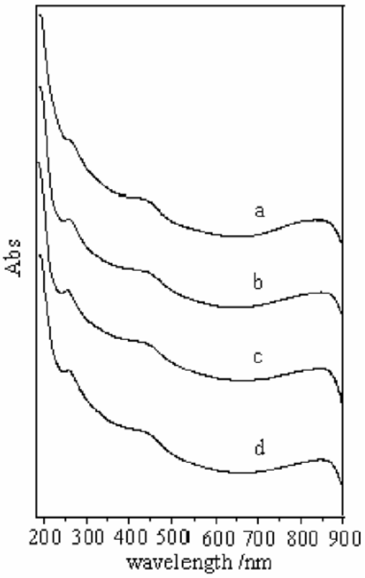

Figure 3. UV–Vis spectra of doped polyaniline (a) α-SiW$_{11}$Fe/PANI, (b) β_1-SiW$_{11}$Fe/PANI, (c) β_2-SiW$_{11}$Fe/PANI, and (d) β_3-SiW$_{11}$Fe/PANI.

Table 2. UV-Vis spectral data of polyaniline/SiW$_{11}$Fe.

Samples	$O_d \rightarrow W$	$O_b/O_c \rightarrow W$	Polaron absorption	
α-SiW$_{11}$Fe/PANI	191	263	440	846
β_1-SiW$_{11}$Fe/PANI	193	262	444	857
β_2-SiW$_{11}$Fe/PANI	191	261	435	850
β_3-SiW$_{11}$Fe/PANI	195	265	446	849
α-SiW$_{11}$Fe	191	253		
β_1-SiW$_{11}$Fe	193	256		
β_2-SiW$_{11}$Fe	191	255		
β_3-SiW$_{11}$Fe	195	254		

absorption band at 440 and 850 nm implies that the PANI has been doped and that its conductivity is increased. Two stronger bands at about 190 and 260 nm appear in UV of polyaniline doped with α, β_i-SiW$_{11}$Fe; the band at 260 nm is characteristic of heteropoly acid, attributed to charge transfer of $O_b/O_c \rightarrow W$ [14]. The bands at 190, 260, 440 and 850 nm show that polyaniline has been protonated by α, β_i-SiW$_{11}$Fe. The UV–Vis absorption spectral data of polyaniline doped with α, β_i-SiW$_{11}$Fe are listed in table 2.

3.3. *XRD spectra*

The X-ray diffraction pattern of the intrinsic polyaniline, β_1-SiW$_{11}$Fe and polyaniline doped with β_1-SiW$_{11}$Fe are shown in figure 4. There are two very broad overlapping halos and some ordered crystalline peaks in the X-ray diffraction pattern of the polyaniline prepared in the presence of β_1-SiW$_{11}$Fe. These peaks are different from those of polyaniline base and β_1-SiW$_{11}$Fe. No peak from the crystalline form of

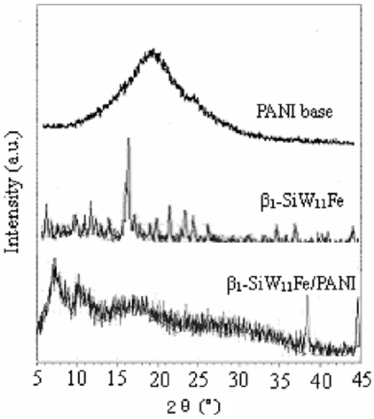

Figure 4. XRD patterns of β_1-SiW$_{11}$Fe, β_1-SiW$_{11}$Fe/PANI and PANI base.

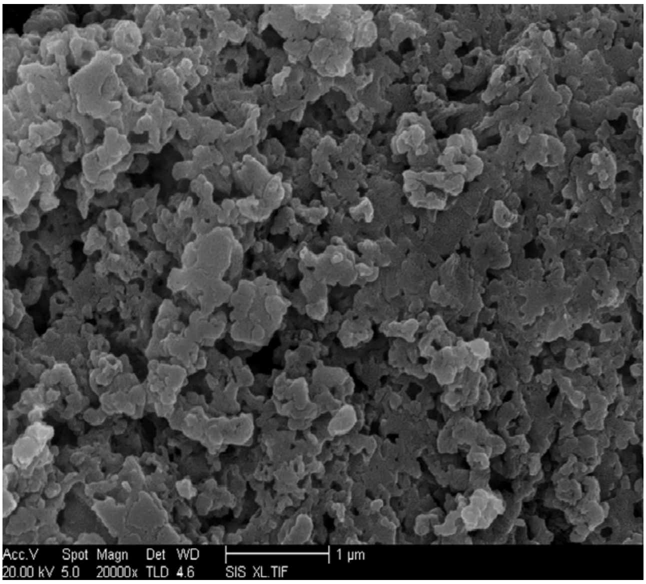

Figure 5. SEM photograph of polyaniline doped with β_1-SiW$_{11}$Fe.

heteropoly acid can be observed, indicating insertion of the heteropoly anion into the polymer matrix. The peak at $2\theta = 7.7^\circ$ ($d = 1.152\,\text{nm}$) is close to the distance of the polymer repeat unit with relatively distinct Bragg reflections, indicating that PANI doped SiW$_{11}$Fe was ordered at short distance.

3.4. *Scanning electron microscopy (SEM)*

Figure 5 shows an SEM photograph of polyaniline doped with β_1-SiW$_{11}$Fe. The image shows the microporous nature of the material. We conclude that the heteropoly acid anions have been incorporated in the bulk of the hybrid material.

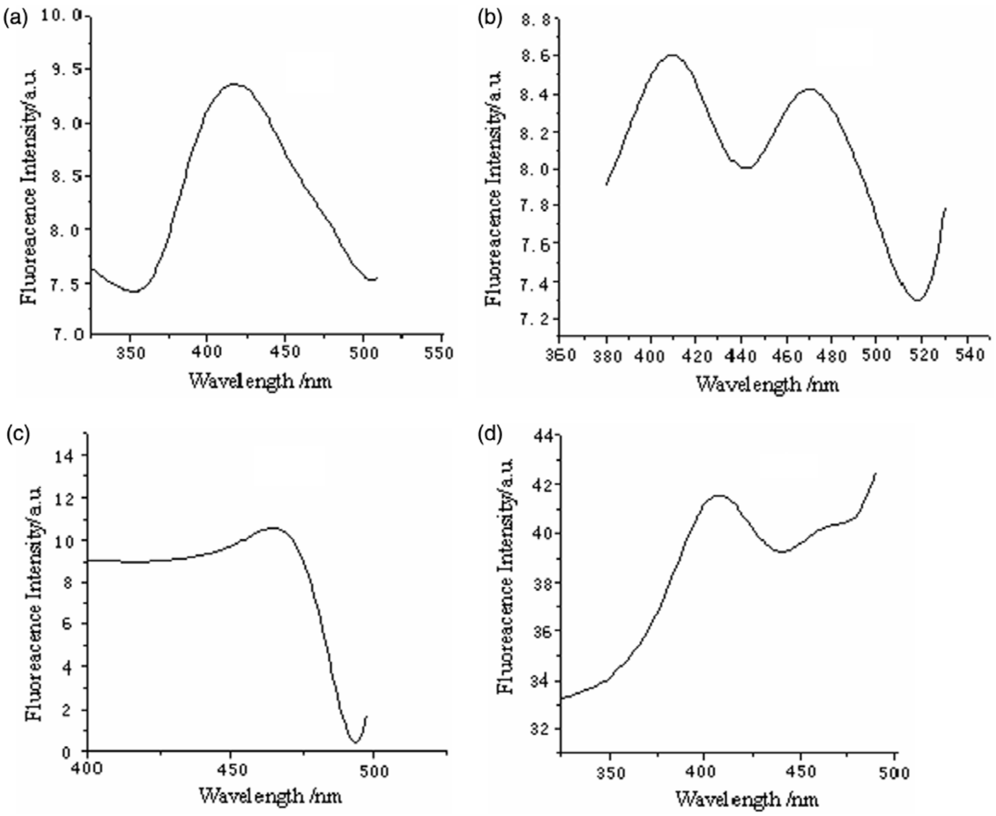

Figure 6. Emission spectra of doped polyaniline (a) α-$SiW_{11}Fe$/PANI (excited at 270 nm), (b) β_1-$SiW_{11}Fe$/PANI (excited at 270 nm), (c) β_2-$SiW_{11}Fe$/PANI (excited at 255 nm), and (d) β_3-$SiW_{11}Fe$/PANI (excited at 250 nm).

3.5. *Fluorescence property*

We monitored the solid materials with the strongest emission wavelength and excited them at the strongest excitation wavelength. Figure 6 gives the fluorescence emission spectra of the polyaniline doped with α, β_i-$SiW_{11}Fe$. For the polyaniline doped with α-$SiW_{11}Fe$, when excited under 270 nm, the material shows broad emission of 350–500 nm with a peak at 418 nm (figure 6a). For polyaniline doped with β_1-$SiW_{11}Fe$, excited at 270 nm, the material shows broad emission of 380–520 nm with peaks at 410 and 470 nm (figure 6b). Polyaniline doped with β_2-$SiW_{11}Fe$, excited at 255 nm, shows broad emission of 425–495 nm with a peak at 466 nm (figure 6c). Polyaniline doped with β_3-$SiW_{11}Fe$, excited at 250 nm, shows broad emission of 350–450 nm with a peak at 465 nm (figure 6d). Because the intrinsic polyaniline has no fluorescence, according to the excitonic luminous mechanism, we conclude that the luminescence comes from the electronic transition between exciton band (produced due to the doping) and valence band [15]. Obviously, the polyaniline molecule synthesized has conjugated transitions; moreover, the rigidity and coplanarity of the polyaniline molecule has been improved.

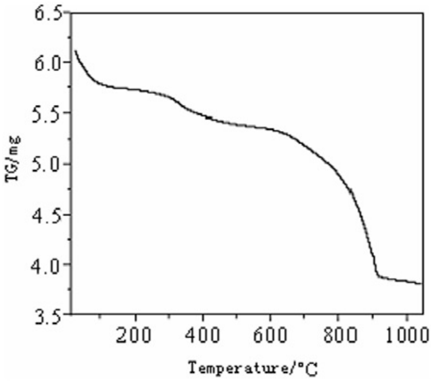

Figure 7. Thermogram of polyaniline doped with β_2-SiW$_{11}$Fe/PANI.

The reason why the α, β_i-SiW$_{11}$Fe/PANI have different emission wavelengths is that the substituted elements in silicotungstate are in different positions, suggesting that changing positions of substituted elements in the silicotungstate may improve the fluorescence of doped polyaniline.

3.6. *Thermal behavior studies*

Figure 7 shows the thermogravimetric measurements in a nitrogen atmosphere of polyaniline doped with β_2-SiW$_{11}$Fe. The TG curve shows that β_2-SiW$_{11}$Fe/PANI undergoes three stages of weight loss, the first stage occurs in the range 27.2–128.1°C with 5.41% mass loss from loss of surface water. The second stage occurs in the range 294.2–508.4°C with 5.60% mass loss from beginning of degradation of polyaniline. The IR spectrum at 300°C is stable (see figure 8b). The third stage occurs in the range 648.5–900°C with 24.37% mass loss, due to degradation of polyaniline backbone and heteropoly acid backbone as indicated by the IR spectrum of the polyaniline, heated at 650°C for 60 min (figure 8c). Figure 9 is the thermogram of the polyaniline base, showing two steps of mass loss; the weight loss at 103.2°C is the loss of surface water and the weight loss at about 241°C is the beginning of degradation of polyaniline. Thermal analysis indicates greater stability of polyaniline doped with β_2-SiW$_{11}$Fe than that of the polyaniline base, with a decomposition temperature at about 53°C higher than that of polyaniline base.

3.7. *Conductivity*

Polyaniline base is insulating with conductivity of the order of 10^{-12} S cm^{-1} [16], and its protonation gives rise to an increase of electronic conductivity several orders of magnitude. HPA is a strong protonic acid that could be doped into the polyaniline base. The protonation occurred at imine nitrogen sites to yield polysemiquinone, in which the polarons delocalized along the polyanaline chain. Usually, the conductivity of polyaniline doped with HPA is 10^{-3}–10^{-6} S cm^{-1} [17]. In order to investigate the effects of iron-substituted silicotungstate isomers on conductivity of the polyaniline, we measured the conductivity of SiW$_{11}$Fe/PANI using a standard four-probe technique.

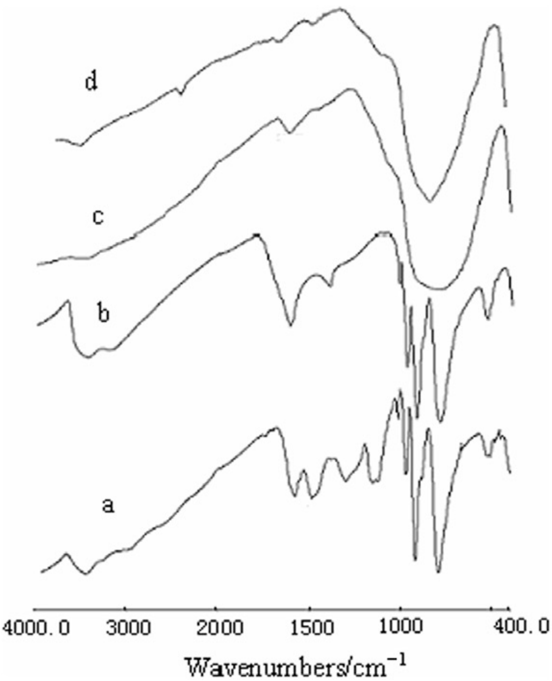

Figure 8. IR spectra of polyaniline doped with β_2-SiW$_{11}$Fe, treated by heating at (a) 120°C, (b) 300°C, (c) 650°C, and (d) 700°C.

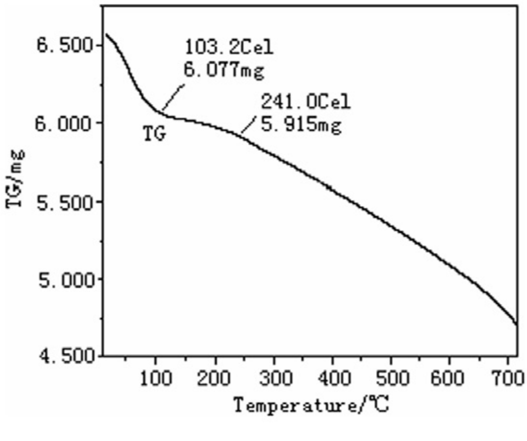

Figure 9. Thermogram of polyaniline base.

The conductivities at room temperature are α-SiW$_{11}$Fe/PANI, $1.02 \times 10^{-2}\,\mathrm{S\,cm^{-1}}$; β_1-SiW$_{11}$Fe/PANI, $8.5 \times 10^{-2}\,\mathrm{S\,cm^{-1}}$; β_2-SiW$_{11}$Fe/PANI, $6.25 \times 10^{-2}\,\mathrm{S\,cm^{-1}}$ and β_3-SiW$_{11}$Fe/PANI, $5 \times 10^{-2}\,\mathrm{S\,cm^{-1}}$, indicating that the materials have good conductivity. The conductivity of polyaniline doped with α, β_i-SiW$_{11}$Fe is higher than that of polyaniline doped with $H_3PMo_{12}O_{40}$ and $H_4PMo_{11}VO_{40}$ ($H_4PMo_{11}VO_{40}$/PANI: $4.78 \times 10^{-4}\,\mathrm{S\,cm^{-1}}$; $H_3PMo_{12}O_{40}$/PANI: $1.34 \times 10^{-2}\,\mathrm{S\,cm^{-1}}$ [15]).

4. Conclusion

Four polyanilines doped with iron-substituted silicotungstate isomers were synthesized by solid-state synthesis. The UV–Vis, IR and XRD results confirm the existence of Keggin anions. The thermal analysis indicates that doping with $SiW_{11}Fe$ gives better thermal stability. The SEM images show that the materials are microporous. The materials exhibit excellent proton conductivity, $8.5 \times 10^{-2}\,S\,cm^{-1}$ at room temperature (20°C). The spectra indicate that polyaniline doped with α, β_i-$SiW_{11}Fe$ have similar fluorescence, $\lambda_{em} = 418$-$470\,nm$, and emit blue light.

Acknowledgements

The financial support from the Science Foundation of the Heilongjiang Provincial Education Department for this work is greatly appreciated.

References

[1] F.C. Wang, R. Yang, J. Gong, C.H. Sui, Y.Q. Luo, L.Y. Qu. *Eur. Polym. J.*, **142**, 2108 (2006).
[2] E.V. Anokhina, A.J. Jacobson. *J. Am. Chem. Soc.*, **126**, 3044 (2004).
[3] A. Tursun, X.G. Zhang, J. Ruxangul. *Mater. Chem. Phys.*, **90**, 367 (2005).
[4] J. Gong, X.J. Cui, Z.W. Xie, S.G. Wang, L.Y. Qu. *Synth. Met.*, **129**, 187 (2002).
[5] A. Tézé, G. Herve. *J. Inorg. Nucl. Chem.*, **39**, 2151 (1977).
[6] A. Tézé, G. Herve. *J. Inorg. Nucl. Chem.*, **39**, 999 (1977).
[7] R.H. Ma, C.T. Liu, L.Y. Qu. *Chin. J. Inorg. Chem.*, **17**, 143 (2001).
[8] L.X. Wang, F.S. Wang. *Acta Polym. Sin.*, **3**, 264 (1989).
[9] L.Y. Qu, R.Q. Lu, J. Peng, Y.G. Chen, Z.M. Dai. *Synth. Met.*, **84**, 135 (1997).
[10] E.-B. Wang, C.-W. Hu, L. Xu. *Introduction to Polyoxometallate Chemistry*, Chemistry Industry Press, Beijing (1998).
[11] J.M. Wilbur, T.C. Sandreczki, I.M. Brown, D.J. Leopold, S. Mohite. *Synth. Met.*, **82**, 175 (1996).
[12] W.S. Huang, A.G. MacDiarmid. *Polymer*, **34**, 1833 (1993).
[13] A. Tursun, X.G. Zhang, J. Ruxangul. *Mat. Chem. Phys.*, **90**, 367 (2005).
[14] J. Gong, Y.G. Chen, L.Y. Qu, Q. Liu. *Polyhedron*, **15**, 2273 (1996).
[15] S.G. Wang, H. He, L.Y. Qu. *Acta Chim. Sin.*, **59**, 1163 (2001).
[16] M. Hasik, W. Turek, E. Stochmal, M. Lapkowski, A. Pron. *J. Catal.*, **147**, 544 (1994).
[17] M. Hasik, J. Pozniczek, A. Pron. *J. Mol. Catal.*, **89**, 329 (1994).